Yielding and rheopexy of aqueous Xanthan gum solutions

E. N'gouamba[1], M. Essadik[1], J. Goyon[1], T. Oerther[2] and P. Coussot[1]

[1]Laboratoire Navier (ENPC-University Gustave Eiffel-CNRS), 77420 Champs sur Marne, France

[2]Bruker BioSpin GmbH, Silberstreifen 4, 76287 Rheinstetten, Germany

Abstract: Xanthan gum (XG) is widely used in cosmetic and pharmaceutic products (creams, pastes) and in oil industry (drilling fluids) as a stabilizing and/or thickening agent. In literature its rheological behavior is mainly presented as that of a shear-thinning or a yield stress fluid. Here, in order to clarify this rheological behavior we study in detail the flow characteristics during continued flow under given conditions (i.e. controlled stress) for a mass concentration ranging from 0.2 to 5 **%.** We are thus able to identify the apparent flow curve of the material after short flow duration and the flow curve in steady state (i.e. after long flow duration). The validity of this flow curve, determined from standard rheometry, is confirmed by Magnetic Resonance velocimetry. These materials start to exhibit a yield stress behavior beyond some critical Xanthan or salt concentration. In that case, a significant increase (by a factor up to 5) of the apparent viscosity is observed during flow in some range of stresses, before reaching steady state. This original rheopectic effect might be due, after some time of flow associated with deformation and reconfiguration of the XG molecules, to the progressive formation of intermolecular links such as hydrogen bonds and/or intermolecular association due to acetate residues.

1. Introduction

Xanthan gum (XG) is a very high molecular weight polysaccharide (with a typical of value of 2×10^6 g/mol) (Jindal & Singh Khattar, 2018), which is widely used in cosmetic and pharmaceutic products (creams, pastes) and in oil industry (drilling fluids) as a stabilizing and/or thickening agent (Candido da Silva et al., 2017; Hublik, 2012; Palaniraj & Jayaraman, 2011). XG is even more used, possibly combined with another hydrocolloid (guar gum, locust bean gum) as an additive in food industry, to gel, stabilize or increase the viscosity of soups, dressings, beverages, baked products, etc. There seems to be no consensus on the exact mechanisms at the origin of these gelling or stabilizing properties, which is certainly in part due to the fact that rheophysical properties of xanthan gum solutions in water are not so well known. In particular, the question arises as to whether the stability of the mixtures is due to the high fluid viscosity induced by the dispersion of macromolecules, the existence of a network of xanthan macromolecules links, or some interaction between the other suspended elements and the xanthan gum molecules inducing a yield stress (Cao et al., 1990; Doublier et al., 2002; Giboreau et al., 1994; Parker et al., 1995).

In contrast with standard polysaccharides which present classic behavior as shear-thinning and strong dependence of viscoelastic properties with angular frequency, XG generally shows a strong shear thinning behavior even at low concentration, and only a slight dependence of viscoelastic properties with frequency for high concentration. These exceptional properties of XG have been thoroughly shown in literature leading to describe XG solutions in water as "weak gels" (Clark & Ross-Murphy, 1987; Doublier et al., 2002; Giboreau et al., 1994). This weak gel behavior is generally attributed to XG molecules which, in contrast to flexible molecules of standard polysaccharides, are ordered and semi-rigid with a helicoidal structure. Thus, at sufficient concentration they do not present an entanglement network as standard polysaccharides (Clark & Ross-Murphy, 1987) but some jammed structure whose mechanical properties depend much on this jamming.

It has long been recognized that xanthan gum solutions are shear-thinning materials whose apparent viscosity increases with the xanthan concentration (Song et al., 2006; Zhong et al., 2013). This was observed through the increase of the stress level in flow curve for a given shear rate or directly by the increase of the viscosity. Also, the effects of temperature and salt addition was studied (Reinoso et al., 2019; Wyatt & Liberatore, 2009; Zhong et al., 2013). A systematic study of the effects of these parameters providing interesting temperature-

concentration-shear intensity equivalences, through the evidence of master curves with an appropriate scaling of the variables (Choppe et al., 2010). The question of the existence of a yield stress often emerges when the concentration is sufficiently increased. Some authors tend to consider that they do not exhibit a yield stress, and only a shear-thinning behavior more marked for higher concentration (Parker et al., 1995) with a Newtonian plateau at low shear rates (Giboreau et al., 1994; Wyatt & Liberatore, 2009) of level also increasing with concentration. Other authors consider the material exhibit a true yield stress (Whitcomb & Macosko, 1978), often from rough studies in a limited range of shear rates(Khalil & Jan, 2012; Rodríguez de Castro et al., 2018), and in general beyond some critical concentration(Dakhil et al., 2019; Song et al., 2006), which was associated with a sufficient number of hydrogen bonds (Song et al., 2006). Finally various techniques for obtaining the yield stress were explored by Ong, which do not always give consistent results, and some thixotropic behavior was suggested (Ong et al., 2019), showing that more studies are needed to clarify the steady state and transient flow properties of these materials.

Indeed, various problems may be observed in some previous studies, such as: measurements in a limited range of shear rates, from which pseudoplastic and yield stress fluid behavior types cannot easily be distinguished; measurements with smooth surfaces, allowing wall slip especially at low shear rates, so that yielding does not appear(Cloitre & Bonnecaze, 2017; Zhang et al., 2017); fast ramps of stress or shear rates, which do not allow to observe steady states. Here we intend to clarify the rheological behavior of xanthan solutions with the help of specific knowledge for the proper characterization of yield stress fluids (Bonn et al., 2017; Coussot, 2005; Ovarlez, 2011) and in large range of concentration, in order to see the possible behavior transition, in the spirit of Song work (Song et al., 2006), but in a wider range and with a more careful observation of transient and steady regimes. This is achieved essentially by using creep tests over sufficient time for large deformation and steady state flow to be reached. The steady state flow characteristics were also ascertained thanks to MRI (Magnetic Resonance Imaging) rheometry tests. This makes it possible to observe the existence of a true yield stress beyond some concentration, and two regimes of behavior in the liquid regime. We start by presenting the materials and procedures, then we present and discuss the data.

2. Materials and methods

Solution preparation

We used a commercial food grade XG powder from *Aroma Zone* (France) to prepare various mass fractions (range between 0.2% and 5%) of aqueous XG solutions. The powder is dispersed in deionized water at room temperature (20°C) and mixed thoroughly with a paddle stirrer at 2000 rpm for 30 min. The solutions is then left at rest for one night to hydrate and the experiments are performed the following day. Prior to any measurement the samples are centrifuged (1000 times the gravity) in order to get rid of air bubbles. $CaCl_2$ (Fisher Scientific) has been also used to study the impact of the salt concentration on the rheological behaviour. In this case, the desired amount of $CaCl_2$ solution 1 M was added during the stirring.

Rheometry

Most of the rheological tests are performed with a stress controlled-rheometer (*Malvern Kinexus*), equipped with a cone and plate geometry of diameter 50 mm and an angle of 1 degree which insures the homogeneity of the stress into the sample. In order to check that some artefacts (evaporation, wall slip, etc) did not affect the results we also carried out some tests with a Couette geometry with serrated wall surfaces, inner diameter and height of 25 mm and 37.5 mm. The rheological measurements, performed under the same conditions

were almost identical for both geometries. This independence of the results with regards to the geometry has also been checked through tests with parallel disks geometries.

Most rheological studies of aqueous XG solutions tend to consider that they are mainly insensitive to their flow history, but some slightly thixotropic (slight evolution of the viscosity with the flow duration has been reported in some case (Ong et al., 2019)). In order to clarify this point, we set up a protocol in which we control carefully the history of the material: a preshear (100 s^{-1} during 60 s), is applied prior to any measurement, in order to erase the flow history, which brings the sample in a reference state. Then the material is left at rest during a certain amount of time (typically 10 s), which potentially allows the structure of the material to rebuild from this reference state (N'gouamba et al., 2020). We checked that this procedure ensures a good reproducibility of the initial state of the solutions and we did not observe aging effect most of the time even though some negligible increase of elastic modulus have been observed when we added salt. Various rheometrical procedures (increasing-decreasing stress ramps, creep tests, oscillations) have been used which are described in the Experimental Section.

MRI velocimetry

MRI (Magnetic Resonance Imaging) velocimetry measurements in Couette cell have been carried out in a *Bruker Biospin GmbH*. The NMR method for the velocity measurement is a "Pulsed Gradient Spin Echo Velocity Imaging" sequence, generating 2D spatially resolved velocity maps from which 1D velocity profiles across the gap of the Couette cell are extracted. The Couette cell characteristics is the following: the inner cylinder, made of polyether ether ketone (PEEK), has a diameter of 14 mm and a length (*H*) of 60 mm, the gap size is e = 2 mm. The inner cylinder is mounted to a motor, the rotation velocity was varied in the range 10 to 600 rpm with a radial resolution of 55 µm. The outer cup is kept static. The Couette cell is immerged into a static field of 300 MHz (7 T). In the plane perpendicular to the axis of the cylinder, the acquisition window is a parallelogram of radial length 7 mm, tangential width 18 mm.

The local flow curve of the material is deduced from the orthoradial velocity (v_θ) profiles measured by NMR velocimetry (see above). The local shear rate at a distance *r* from the central axis writes $\dot{\gamma} = \frac{v_\theta}{r} - \frac{dv_\theta}{dr}$. The local shear stress at the same distance *r* is deduced from torque (*T*) measurements (with the conventional rheometer under exactly same flow conditions) according to $\tau = \frac{T}{2\pi H r^2}$.

3. Results and discussion

As a first approach of the rheological behavior of XG we look at data obtained from sweep tests under controlled stress at different concentrations. Here we imposed stress ramps with logarithmically increasing stress over a total duration of 120 s for each ramp. Thus, in such a test a steady state at each given stress value is not necessarily reached. The increasing and decreasing stress curves very well superimpose between 0.1 s^{-1} and the largest shear rate reached, typically a few thousands s^{-1} (see Figure 1), which tends to suggest that steady state flow is reached in this range. For lower shear rates the stress curve for the decreasing ramp is situated above the increasing ramp curve. This is reminiscent of the behavior observed for yield stress fluids (Coussot, 2005) for which, in such a test, the fast increase of the stress corresponds to the progressively increasing deformation (as a result of the ramp) in the solid regime, before reaching the plateau associated with the transition to the liquid regime then flow in this regime. Here this effect is minor at small concentrations and progressively becomes quite clear and similar to that observed for well-known yield stress

fluids. This is consistent with a pseudoplastic behavior at small concentration, becoming yield stress behavior beyond some concentration.

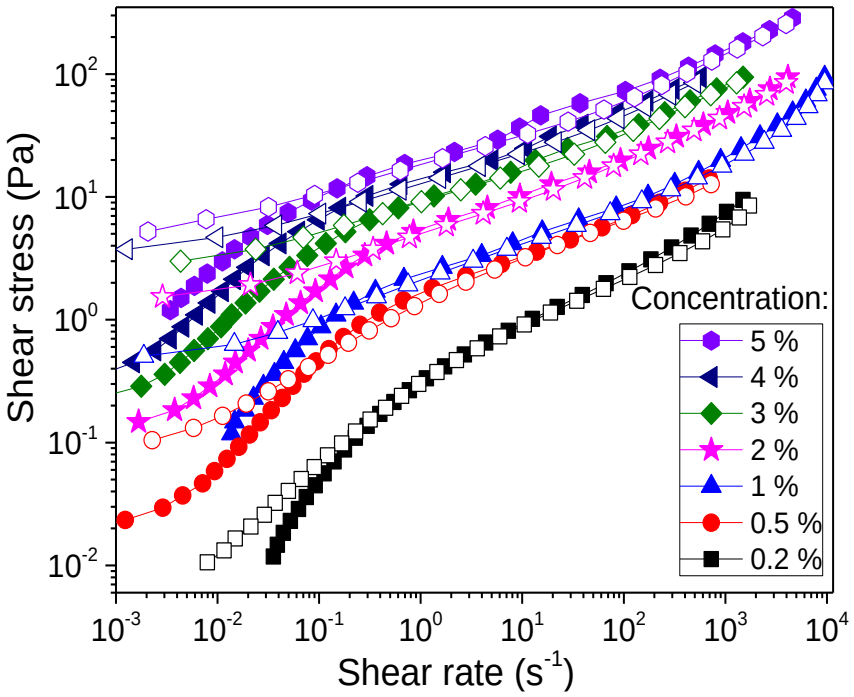

Figure 1. Sweep stress tests for various mass concentrations of aqueous xanthan gum at 25°C. Increasing ramp (filled symbols) and decreasing ramp (open symbols).

Such a description is also consistent with the characteristics of the elastic and loss moduli variations for amplitude ramps (see Figure 2). Here we performed sweep strain tests at a frequency of 1 Hz, for the same range of concentrations. For low concentrations, the elastic and viscous moduli are almost equal at small deformations, indicating a material in which elastic and viscous effects are both important, while the elastic modulus drops for deformation larger than about 1, which means that the material tends to a simple viscous behavior. As the concentration is increased the elastic to viscous modulus ratio progressively increases at low deformation, indicating that the elasticity becomes dominant in this regime, while the elastic modulus drops and the viscous modulus increases beyond some deformation amplitude, which both correspond to typical characteristics of yield stress fluids (N'gouamba et al., 2019). The transition to a clearly yield stress fluid behavior with the increase of concentration can be considered to be around 1% for both tests (dynamic tests and stress sweep).

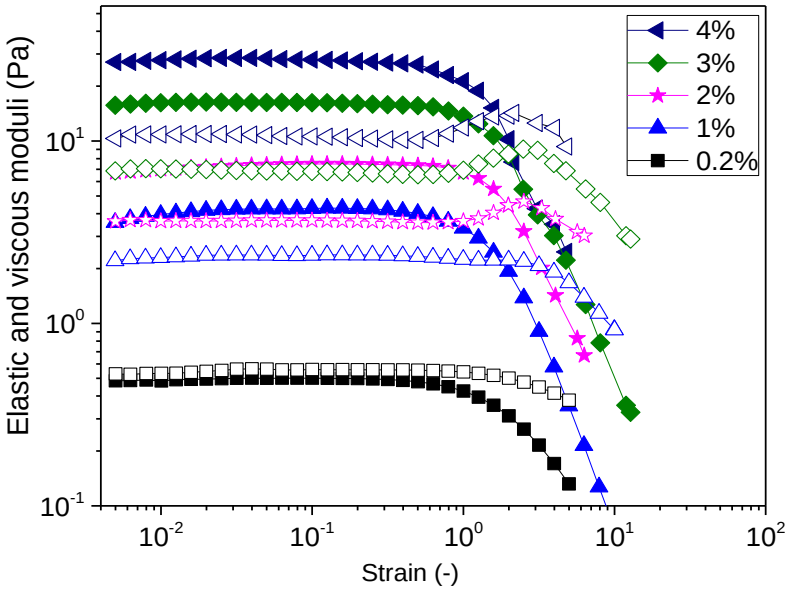

Figure 2. Oscillatory amplitude sweep strain for various concentration at 25°C: Elastic (filled symbols) and viscous (open symbols) moduli.

Adding salt significantly increases the apparent viscosity as already observed in similar XG polyelectrolyte (Wyatt & Liberatore, 2009). More precisely, the salt addition induces an increase of the yield stress of the material (see Figure 3). Remarkably, the flow curves obtained by addition of salt is similar to that obtained without salt by adding a constant stress component (see Figure 3). This means that the addition of salt has simply a "plastic" effect on the energy dissipation, i.e. essentially independent of the shear rate. This fundamentally differs from an effect, as is often observed for a yield stress fluid, of concentration increase, where the stress is approximately multiplied by a factor (see e.g. (Boujlel et al., 2012)). This means that the salt has no direct impact on the jammed structure and the unjamming processes, and no systematic (at all flow rates) impact on the viscous dissipation, it essentially induces an additional interaction between the close elements, which breaks and reforms along the relative motion of the elements. This interaction is likely a reduction of electrostatic repulsion.

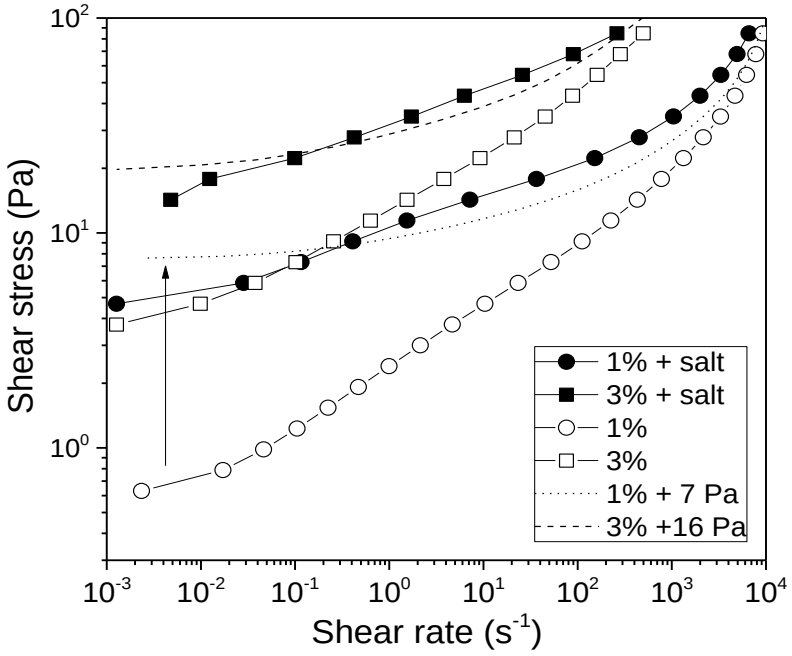

Figure 3. Flow curve (decreasing ramp) of aqueous xanthan gum solutions at different concentrations with (filled symbols) or without (open symbols) added salt ([$CaCl_2$] = 15 mM). The dashed lines correspond to the flow curves without salt, to which a constant stress has been added.

Actually we have no clear evidence that the above flow curves correspond to steady state flows, so that the real existence of a yield stress beyond some concentration is not yet proved. In order to clarify this point we now apply given stress values and follow the evolution of the deformation in time (creep tests). Typical results are shown in Figure 4. For a concentration smaller than 1% a steady state flow is rapidly reached, i.e. the deformation increases linearly in time (see Figure 4a) for any stress level. For a concentration equal or larger than 1%, below a critical stress (about 3 Pa for the example of Figure 4b) the deformation increases much more slowly and its rate of increase continuously decreases. Indeed, we have $\gamma \approx kt^{1/3}$ which implies $\dot{\gamma} \propto t^{-2/3}$, showing that the shear rate tends towards zero for sufficiently long times. Beyond this critical stress, after some time, the deformation increases linearly with time. Under these conditions we have a rheological behavior which resembles that of a yield stress fluid, i.e. with two regimes, one in which the fluid tends to stop flowing, even with some residual flow at rate decreasing in time, and one in which the flow steadily flows.

Actually, we can observe another original trend in these creep tests: in some range of stresses above the yield stress, although the steady state flow seemed to be reached rapidly after the beginning of the test, the flow apparently slow down and finally the deformation reaches a new straight line of slope 1 associated with a flow rate smaller than the initial one (see Figure 4b).

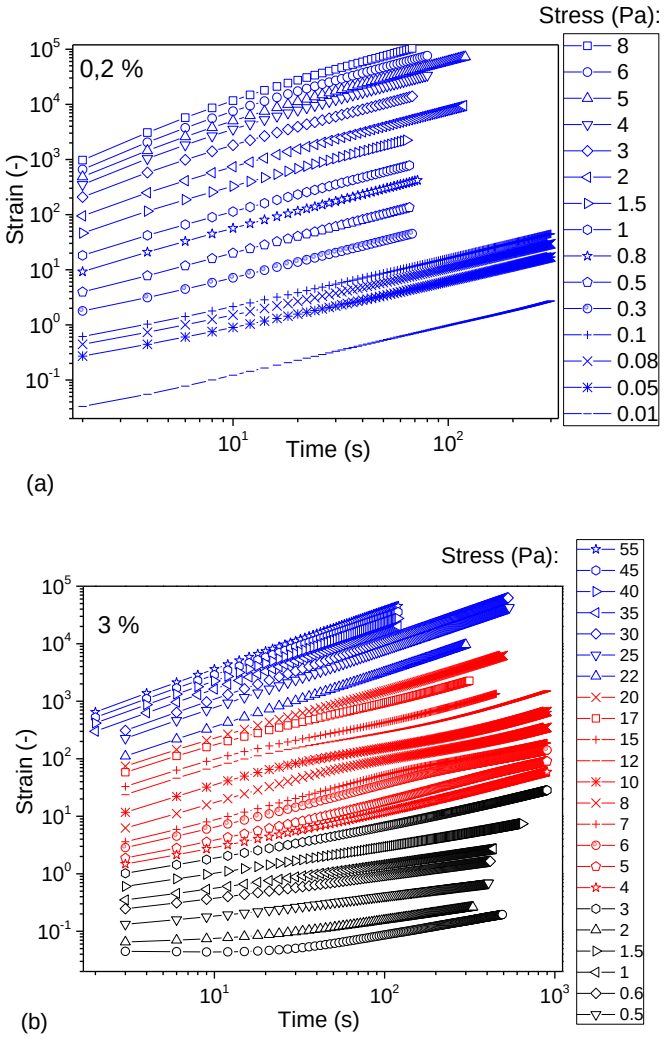

Figure 4. Creep tests for different concentrations of xanthan gum in water ((a) 0.2%; (b) 3%): shear strain vs time for different stress values. Blue symbols correspond to the liquid regime where the steady flow is reached quite instantaneously, red symbols correspond to the liquid regime but with a transient regime, and black symbols correspond to the solid regime with limited deformation.

In order to have a clearer view of this effect we represent the creep tests data in terms of the apparent viscosity as a function of time (see Figure 5a,b,c). The same observations as above obviously emerge: for low concentration the viscosity rapidly reaches a plateau at any stress level (see Figure 5a); we can note however that for stress value below 0.3 Pa the viscosity apparently increases but since we are in the range of low deformation it is not possible to conclude about a slight shear-thickening effect or a tendency to stoppage associated with the existence of a very low yield stress; for concentrations equal or larger than 1% (see Figure 5b,c) the viscosity reaches a plateau for stress values above the yield stress while it tends to infinity for stresses below the yield stress. Let us remark that in some papers, for low concentrations, a viscosity plateau was observed at low shear rates in consistency with the behavior of standard polymer solutions, which appears in contradiction with our data for which even at low stresses the viscosity in steady state increases for stress decrease (see Figures 5a,b). Actually, our creep test data show that this viscosity plateau for XG solutions just corresponds to the transient behavior of the material, and not to the steady state viscosity. Indeed, we can

see in Figure 5a and 5b that for low imposed stress values (less than 0.3 Pa for 0.2% and less than 3 Pa for 1%) the initial viscosity is almost constant, which would give a plateau if represented as a function of the shear rate or shear stress. However, if we then follow this viscosity in time, which is the objective of creep tests over sufficient time, we see that the viscosity increase, and the plateau would disappear. Again, this is consistent with the assumption that jamming effects are dominant on the material behavior.

The most original trend is that for concentration larger than 1%, we can see that in some range of stresses from just above the yield stress (for example between 5 and 22 Pa for 3%), the viscosity starts from a low value, apparently follows a plateau, and at some deformation starts increasing significantly, up to ten times its initial value (see Figure 5c). It is worth emphasizing that this effect is reversible: when one stops the flow and starts again a test with the same sample at the same stress level one obtains the same trend. For larger stress values the viscosity remains approximately constant during the flow.

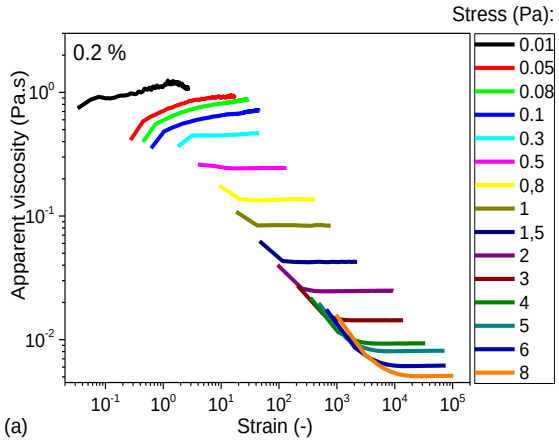

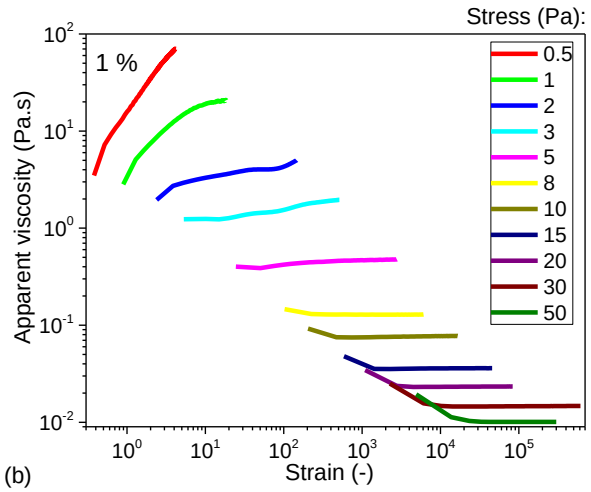

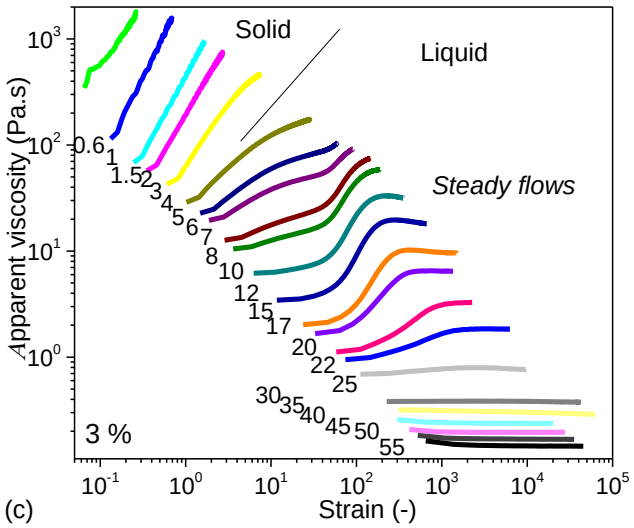

Figure 5. Creep tests for different concentrations of xanthan gum in water ((a) 0.2%; (b) 1%; (c) 3%): apparent viscosity vs strain for different stress values.

It is worth noting that this effect occurs after deformations (say, of the order of 100) much larger than the critical one associated with the solid-liquid transition, which is between 1 and 10 according to creep tests data (see Figure 5). As a consequence, the viscosity increase effect may be considered as rheopexy, in which the material becomes progressively more viscous with flow duration. In this context it is interesting to plot the apparent flow curve of the material at the main steps of the process, namely in the very first time (≈ 2 s) of the flow and in the steady state flow. We then find (see Figure 6) that the fluid apparently exhibits two main flow regimes associated with two different flow curves: initially it flows in the first regime (the lower flow curve) but, below some stress value, after some deformation, it steadily flows in the second regime, while it goes on flowing in the first regime for larger stresses.

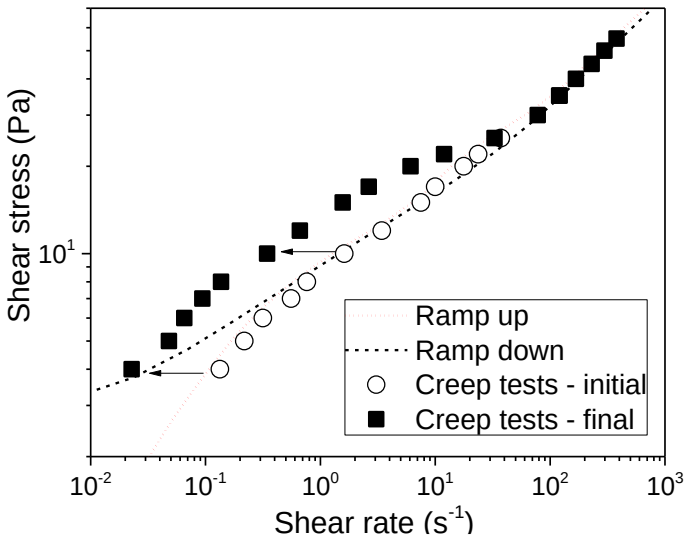

Figure 6. Stress vs shear rate for a XG solution at 3% under different flow conditions: creep tests or sweep tests. Upward and downward ramps correspond to flow curves already plotted in Figure 1.

Such transient effects are often associated with the developments of heterogeneities, either of the fluid component distribution or of the flow characteristics (shear localization). It does not seem possible to have fluid density heterogeneity as at such large concentrations the elements are part of a jammed structure, at the origin of the yield stress. The possibility of shear localization may be clarified from MRI measurements which provide the steady state velocity profiles under different rotation velocities of the inner cylinder (see typical data in Figure 7), from which we can extract the flow properties (see Section 2). For some rotation velocities it seems that wall slip affected the flow but this does not impair the data analysis since we directly measure the flow characteristics inside the sample by MRI velocimetry and the stress imposed is transmitted from the inner to the outer cylinder, whatever the flow characteristics, as long as the gap is filled with fluid. It appears that the flow characteristics perfectly fall along the steady state flow curve obtained from macroscopic tests (see Figure 8a,b). This confirms that the apparent flow characteristics after a sufficiently large flow duration effectively correspond to homogeneous steady state flows.

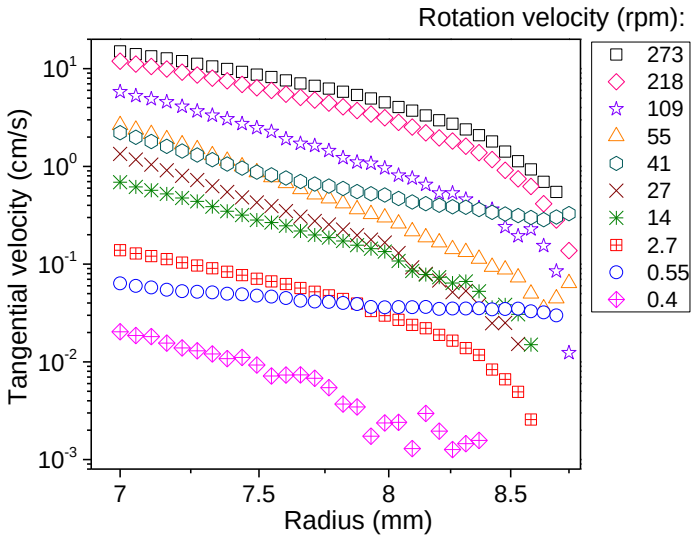

Figure 7. Velocity profiles for steady states flows of a XG solution at 4% in the Couette cell as determined by MRI for different rotation velocities. Note that the apparent shear rate, calculated by dividing the relative tangential velocity by the gap, ranged from 0.14 to 100 s^{-1}.

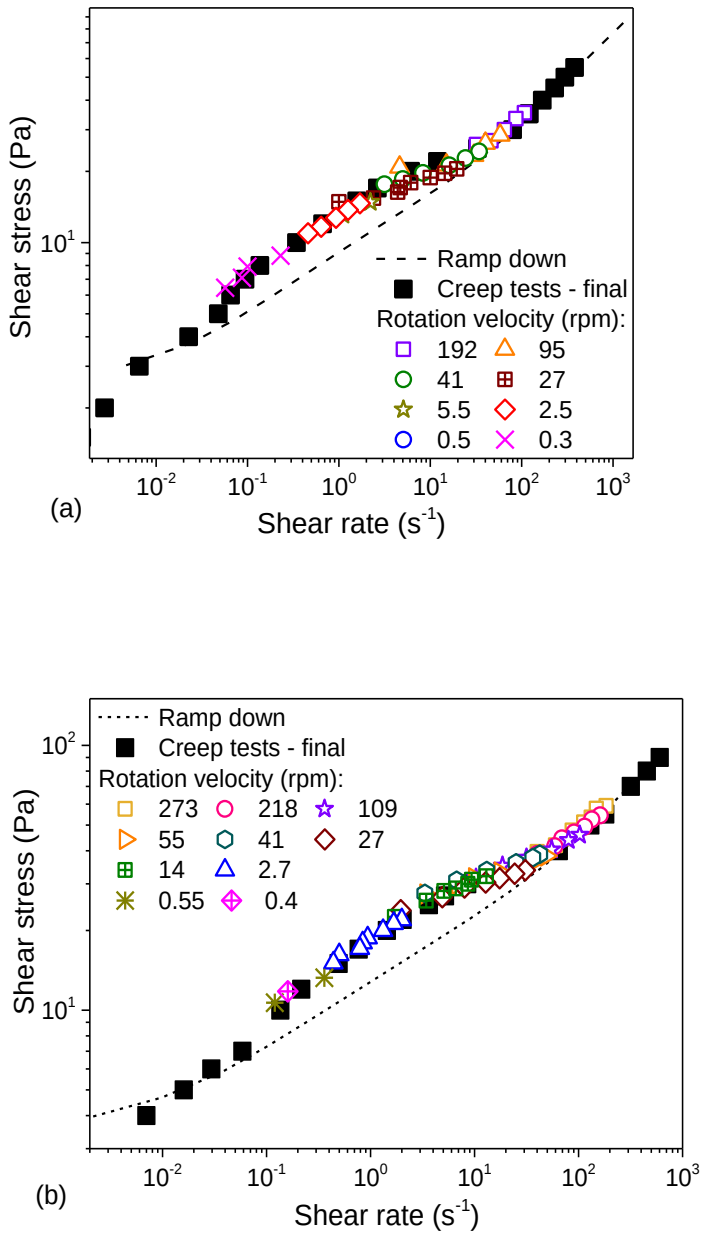

Figure 8. Stress vs shear rate for XG solutions at different concentrations ((a): 3%; (b): 4%) as deduced from creep tests, flow curve in decreasing ramp and local flow characteristics in steady state determined by MRI.

We can finally suggest the following scheme: we are dealing with a material exhibiting a yield stress due to the existence of a jammed structure of elastic XG molecules. When a sufficiently large stress is applied to the material, the structure breaks. This breakage allows the relative motion of the blobs, which corresponds to some viscous behavior. For sufficiently low shear rates, after some time of flow associated with deformation and reconfiguration of the XG molecules, some intermolecular links via hydrogen bonds (Harrison et al., 1999) and/or intermolecular association due to acetate residues (Marcotte et al., 2001) can be reformed, which tend to increase the viscosity. For sufficiently high shear rates this effect would not occur or be negligible.

We thus have a rheopectic fluid whose behavior evolution are essentially governed by flow duration. Indeed, beyond its yield stress, in some range of shear rates, it behaves as low viscous fluid and its viscosity increases in time (during flow) until it reaches steady state; when it is sheared at higher shear rates the viscosity remains low; during an increasing ramp of stress or shear rate over a short time the fluid viscosity remains low (i.e. in

the first regime) (see Figure 6); during a decreasing ramp over a short time, the material remains in its low viscous regime (see Figure 6).

Conclusion

We have studied experimentally the rheological behavior of aqueous Xanthan Gum solutions for different mass and salt concentrations. Unlike most studies on polymer solutions which focus on viscoelastic properties by means of oscillatory shear measurements, here we mainly carried out steady state shear flow measurements. We were thus able to show clearly that for high concentration (above 1%), aqueous XG solution exhibit a true yield stress unlike most macromolecular solutions. However, our investigation of the liquid regime in the steady state reveals that, for low values of shear stress, these XG solutions present a striking rheopectic behavior, i.e., and increase of the apparent viscosity with time for a given shear stress. The validity of our rheological measurements by mean of conventional rheometry, was checked by MRI velocimetry in order to ensure that this effect was not associated with some artefact such as shear localization. We thus suggest a scenario in which the intermolecular interactions (hydrogen bonds or association due to acetate residues) of XG molecules, at high concentration can be reformed for low value of shear stress in the liquid regime.

This study allows thus to clarify the behavior of XG solution in their liquid regime, which is of significant interest for the various applications in food, cosmetic and drilling, etc. Thus, we emphasize the importance of studying in detail the “true” steady state flow characteristics of materials, through continued flows.

Future possible work could attempt to describe more quantitatively the role of the reformation of intermolecular bonds in the rheopexy. This may require coupling rheological tests with some structural measurements such as small angle x-ray or neutron scattering

Acknowledgement

The authors acknowledge the support of the French National Research Agency within the frame of the grant ANR-17-CE05-0023-04.

Conflict of Interests: The authors declare no conflicts of interest.

Appendix

Additional rheological data for 3% and 4% XG solutions

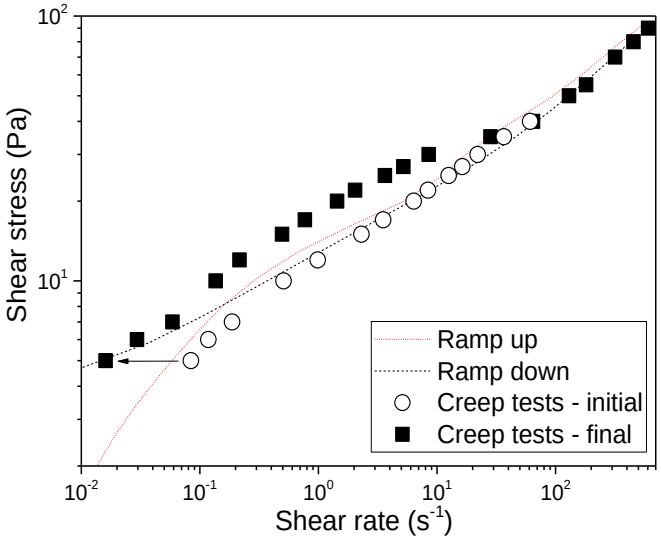

Figure 10. Stress vs shear rate for a XG solution at 4% under different flow conditions: creep tests or sweep tests.

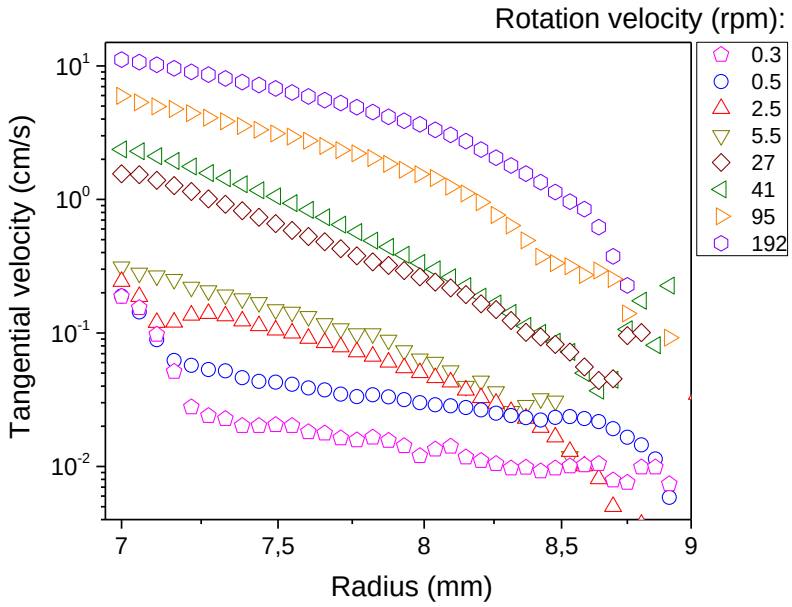

Figure 11. Velocity profiles for steady states flows of a XG suspension at 3% in the Couette cell as determined by MRI for different rotation velocities. Note that the apparent shear rate, calculated by dividing the relative tangential velocity by the gap, ranged from 0.1 to 70 s^{-1}.

Bibliography

Bonn, D., Denn, M. M., Berthier, L., Divoux, T., & Manneville, S. (2017). Yield stress materials in soft condensed matter. *Reviews of Modern Physics*, *89*(3), 1–40.

https://doi.org/10.1103/RevModPhys.89.035005

Boujlel, J., Maillard, M., Lindner, A., Ovarlez, G., Chateau, X., & Coussot, P. (2012). Boundary layer in pastes—Displacement of a long object through a yield stress fluid. *Journal of Rheology*, *56*(5), 1083–1108. https://doi.org/10.1122/1.4720387

Candido da Silva, L. C., Targino, B. N., Furtado, M. M., de Oliveira Pinto, M. A., Rodarte, M. P., & Hungaro, H. M. (2017). Xanthan: Biotechnological Production and Applications. In *Microbial Production of Food Ingredients and Additives* (Vol. 2020). Elsevier Inc. https://doi.org/10.1016/b978-0-12-811520-6.00013-1

Cao, Y., Dickinson, E., & Wedlock, D. J. (1990). Creaming and flocculation in emulsions containing polysaccharide. *Topics in Catalysis*, *4*(3), 185–195. https://doi.org/10.1016/S0268-005X(09)80151-3

Choppe, E., Puaud, F., Nicolai, T., & Benyahia, L. (2010). Rheology of xanthan solutions as a function of temperature , concentration and ionic strength. *Carbohydrate Polymers*, *82*(4), 1228–1235. https://doi.org/10.1016/j.carbpol.2010.06.056

Clark, A. H., & Ross-Murphy, S. B. (1987). Structural and Mechanical Properties of Biopolymer Gels. *Advances in Polymer Science*, *83*, 60–192.

Cloitre, M., & Bonnecaze, R. T. (2017). A review on wall slip in high solid dispersions. *Rheologica Acta*, *56*, 283–305. https://doi.org/10.1007/s00397-017-1002-7

Coussot, P. (2005). *Rheometry of pastes, suspensions, and granular materials: applications in industry and environment* (Jhon Wiley).

Dakhil, H., Auhl, D., & Wierschem, A. (2019). Infinite-shear viscosity plateau of salt-free aqueous xanthan solutions. *Journal of Rheology*, *63*(1), 63–69. https://doi.org/10.1122/1.5044732

Doublier, J.-L., Maingonnat, J.-F., & Cuvelier, G. (2002). Des sauces aux émulsions alimentaires. In *Comprendre la Rhéologie : De la circulation du sang à la prise du béton* (EDP Scienc, pp. 116–136).

GIBOREAU, A., CUVELIER, G., & LAUNAY, B. (1994). Rheological Behaviour of Three Biopolymer/Water Systems, With Emphasis on Yield Stress and Viscoelastic Properties. *Journal of Texture Studies*, *25*(2), 119–138. https://doi.org/10.1111/j.1745-4603.1994.tb01321.x

Harrison, G., Franks, G. V, Tirtaatmadja, V., & Boger, D. V. (1999). Suspensions and polymers - Common links in rheology. *Korea-Australia Rheology Journal*, *11*(3), 197–218.

Hublik, G. (2012). Xanthan gum. *Polymer Science: A Comprehensive Reference, 10 Volume Set*, *10*, 221–229. https://doi.org/10.1016/B978-0-444-53349-4.00262-4

Jindal, N., & Singh Khattar, J. (2018). Microbial Polysaccharides in Food Industry. In *Biopolymers for Food Design*. Elsevier Inc. https://doi.org/10.1016/B978-0-12-811449-0.00004-9

Khalil, M., & Jan, B. M. (2012). Herschel-Bulkley Rheological Parameters of a Novel Environmentally Friendly Lightweight Biopolymer Drilling Fluid from Xanthan Gum and Starch. *Journal of Applied Polymer Science*, *124*, 595–606. https://doi.org/10.1002/app

Marcotte, M., Hoshahili, A. R. T., & Ramaswamy, H. S. (2001). Rheological properties of selected hydrocolloids as a function of concentration and temperature. *Food Research International*, *34*(8), 695–703. https://doi.org/10.1016/S0963-9969(01)00091-6

N'gouamba, E., Goyon, J., & Coussot, P. (2019). Elastoplastic behavior of yield stress fluids. *Physical Review Fluids*, *4*(12), 123301. https://doi.org/10.1103/PhysRevFluids.4.123301

N'gouamba, E., Goyon, J., Tocquer, L., Oerther, T., & Coussot, P. (2020). Yielding , thixotropy , and strain

stiffening of aqueous carbon black suspensions. *Journal of Rheology*, *64*, 955. https://doi.org/10.1122/8.0000028

Ong, E. E. S., O'Byrne, S., & Liow, J. L. (2019). Yield stress measurement of a thixotropic colloid. *Rheologica Acta*, *58*(6–7), 383–401. https://doi.org/10.1007/s00397-019-01154-y

Ovarlez, G. (2011). Caractérisation rhéologique des fluides à seuil. *Rhéologie*, *20*, 28–43.

Palaniraj, A., & Jayaraman, V. (2011). Production, recovery and applications of xanthan gum by Xanthomonas campestris. *Journal of Food Engineering*, *106*(1), 1–12. https://doi.org/10.1016/j.jfoodeng.2011.03.035

Parker, A., Gunning, P. A., Ng, K., & Robins, M. M. (1995). How does xanthan stabilize salad dressing? *Food Hydrocolloids*, *9*(4), 333–342. https://doi.org/10.1016/S0268-005X(09)80263-4

Reinoso, D., Martín-Alfonso, M. J., Luckham, P. F., & Martínez-Boza, F. J. (2019). Rheological characterisation of xanthan gum in brine solutions at high temperature. *Carbohydrate Polymers*, *203*(June 2018), 103–109. https://doi.org/10.1016/j.carbpol.2018.09.034

Rodríguez de Castro, A., Ahmadi-Sénichault, A., & Omari, A. (2018). Using Xanthan Gum Solutions to Characterize Porous Media with the Yield Stress Fluid Porosimetry Method: Robustness of the Method and Effects of Polymer Concentration. *Transport in Porous Media*, *122*(2), 357–374. https://doi.org/10.1007/s11242-018-1011-8

Song, K. W., Kim, Y. S., & Chang, G. S. (2006). Rheology of concentrated xanthan gum solutions: Steady shear flow behavior. *Fibers and Polymers*, *7*(2), 129–138. https://doi.org/10.1007/BF02908257

Whitcomb, P. J., & Macosko, C. W. (1978). Rheology of Xanthan Gum. *Journal of Rheology*, *22*(5), 493–505. https://doi.org/10.1122/1.549485

Wyatt, N. B., & Liberatore, M. W. (2009). Rheology and Viscosity Scaling of the Polyelectrolyte Xanthan Gum. *Journal of Applied Polymer Science*, *114*(6), 4076–4084. https://doi.org/10.1002/app

Zhang, X., Lorenceau, E., Basset, P., Bourouina, T., Rouyer, F., Goyon, J., & Coussot, P. (2017). Wall Slip of Soft-Jammed Systems : A Generic Simple Shear Process. *Physical Review Letters*, *119*, 208004. https://doi.org/10.1103/PhysRevLett.119.208004

Zhong, L., Oostrom, M., Truex, M. J., Vermeul, V. R., & Szecsody, J. E. (2013). Rheological behavior of xanthan gum solution related to shear thinning fluid delivery for subsurface remediation. *Journal of Hazardous Materials*, *244–245*(November), 160–170. https://doi.org/10.1016/j.jhazmat.2012.11.028